Figure 1

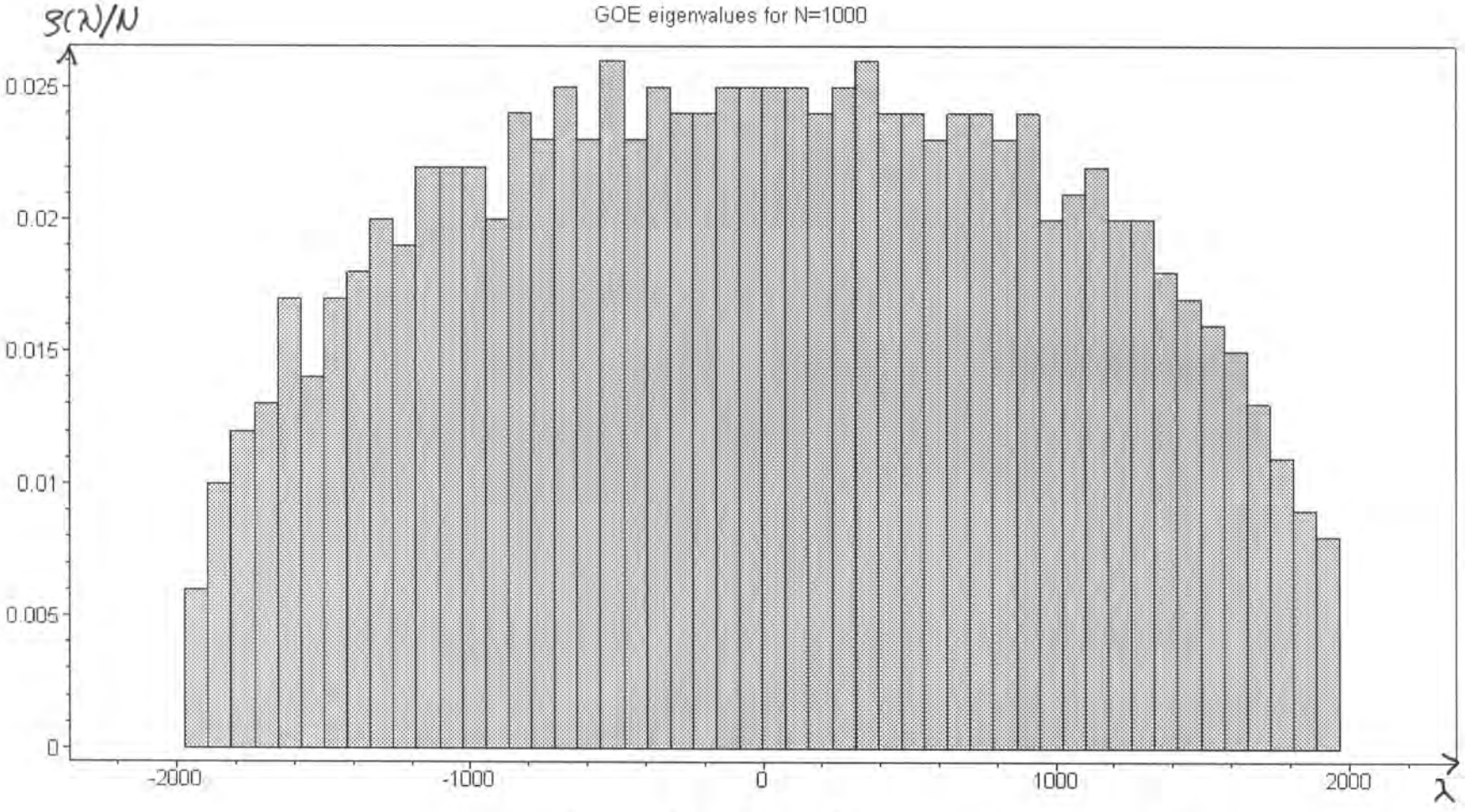


Eigenvalue density of a $N \times N$ matrix in the GOE ensemble, $N = 1000$.

Figure 2

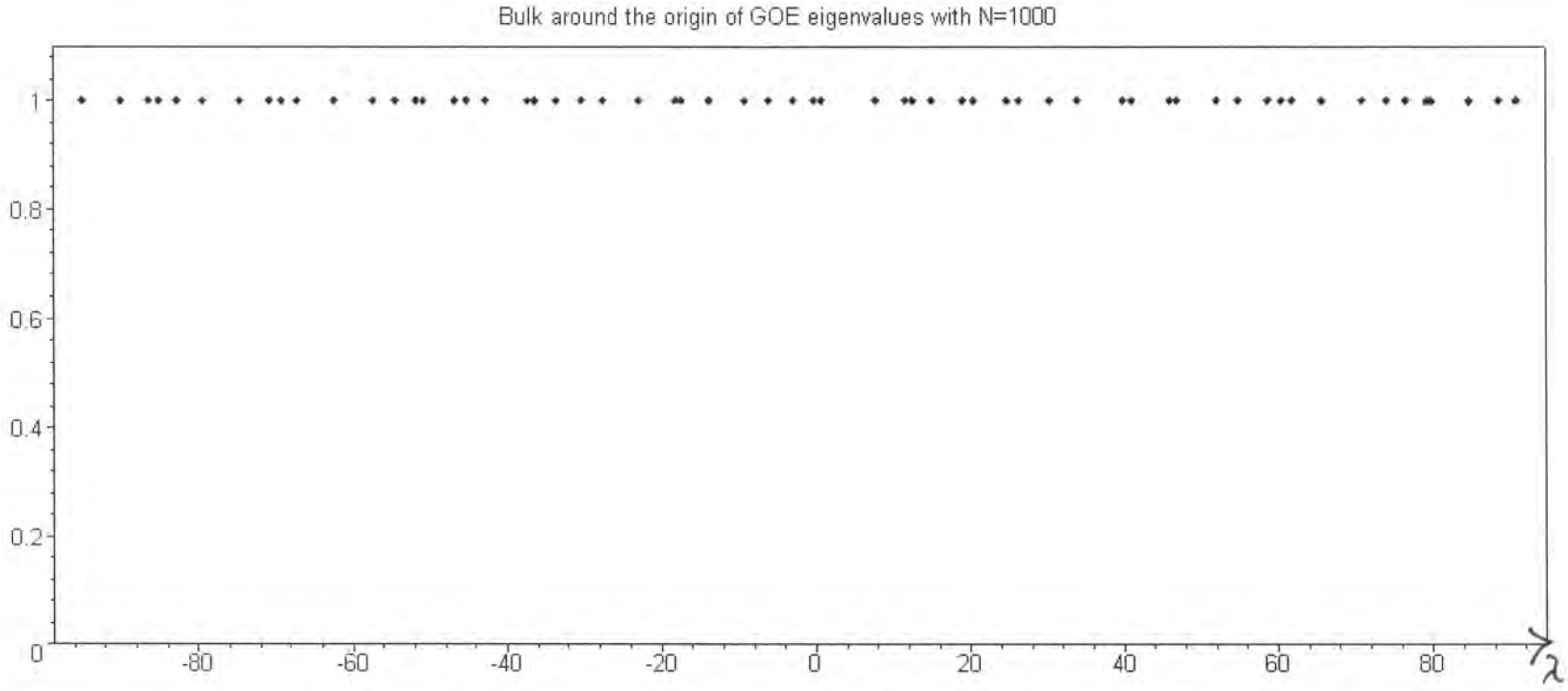


Eigenvalues in the bulk of the $N \times N$ GOE matrix, $N = 1000$,

Figure 3

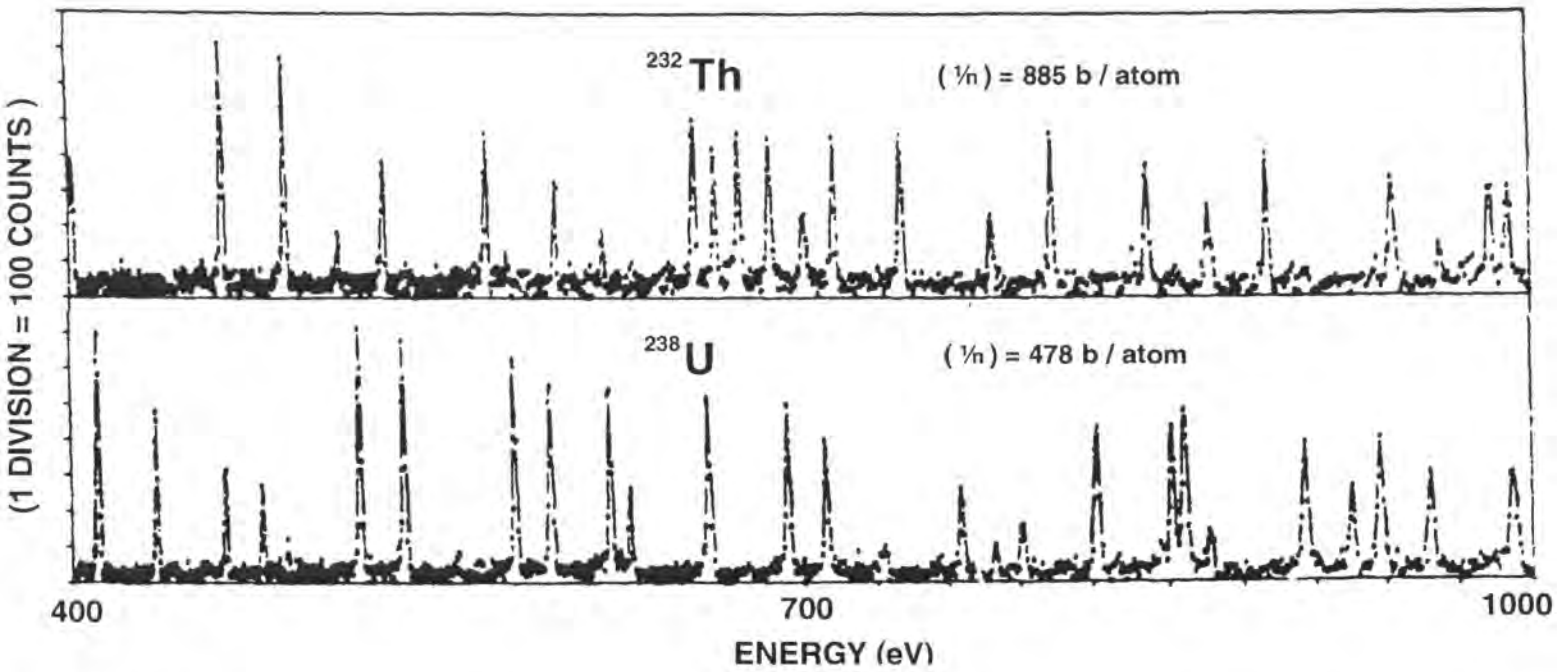


**Figure 1.1.** Slow neutron resonance cross-sections on thorium 232 and uranium 238 nuclei. Reprinted with permission from The American Physical Society, Rahn et al., Neutron resonance spectroscopy, X, *Phys. Rev. C* 6, 1854–1869 (1972).

.Taken from Mehta book "Random Matrices", page 2.

Figure 4.1

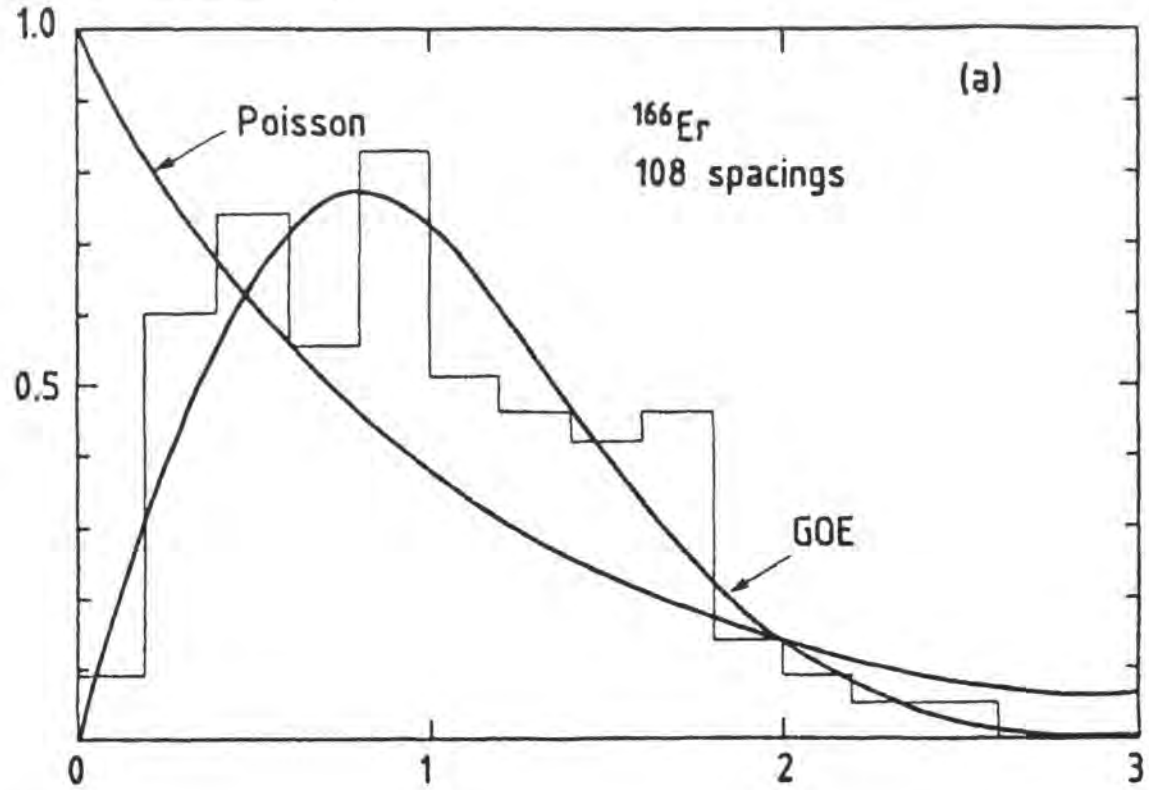


**Figure 1.3.** The probability density for the nearest neighbor spacings in slow neutron resonance levels of erbium 166 nucleus. The histogram shows the first 108 levels observed. The solid curves correspond to the Poisson distribution, i.e. no correlations at all, and that for the eigenvalues of a real symmetric random matrix taken from the Gaussian orthogonal ensemble (GOE). Reprinted with permission from The American Physical Society, Liou et al., Neutron resonance spectroscopy data, *Phys. Rev. C* 5 (1972) 974–1001.

.Mehta book, page 12.

Figure 4.2

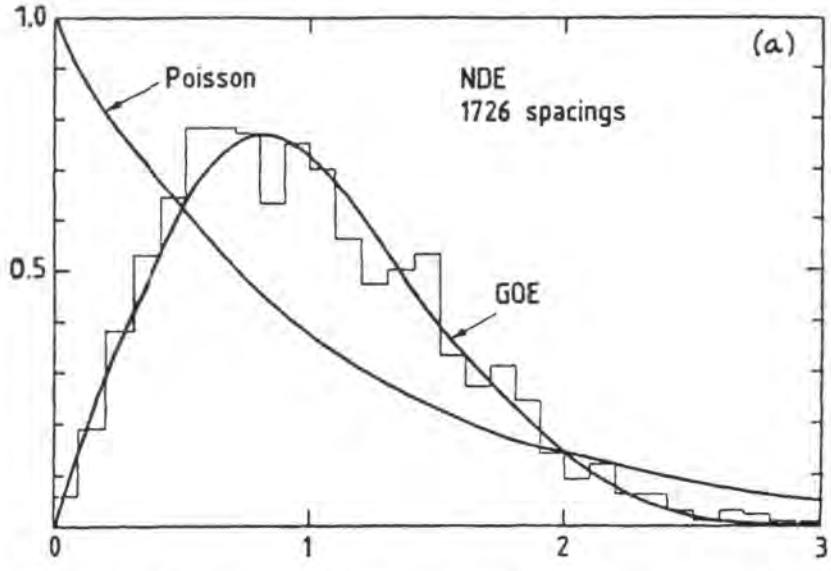


**Figure 1.4.** Level spacing histogram for a large set of nuclear levels, often referred to as nuclear data ensemble. The data considered consists of 1407 resonance levels belonging to 30 sequences of 27 different nuclei: (i) slow neutron resonances of Cd(110, 112, 114), Sm(152, 154), Gd(154, 156, 158, 160), Dy(160, 162, 164), Er(166, 168, 170), Yb(172, 174, 176), W(182, 184, 186), Th(232) and U(238); (1146 levels); (ii) proton resonances of Ca(44) ($J = 1/2+$), Ca(44) ($J = 1/2-$), and Ti(48) ($J = 1/2+$); (157 levels); and (iii) $(n, \gamma)$-reaction data on Hf(177) ($J = 3$), Hf(177) ($J = 4$), Hf(179) ($J = 4$), and Hf(179) ($J = 5$); (104 levels). The data chosen in each sequence is believed to be complete (no missing levels) and pure (the same angular momentum and parity). For each of the 30 sequences the average quantities (e.g. the mean spacing, spacing/mean spacing, number variance $\mu_2$, etc., see Chapter 16) are computed separately and their aggregate is taken weighted according to the size of each sequence. The solid curves correspond to the Poisson distribution, i.e. no correlations at all, and that for the eigenvalues of a real symmetric random matrix taken from the Gaussian orthogonal ensemble (GOE). Reprinted with permission from Kluwer Academic Publishers, Bohigas O., Haq R.U. and Pandey A., Fluctuation properties of nuclear energy levels and widths, comparison of theory with experiment, in: *Nuclear Data for Science and Technology*, Bökhoff K.H. (Ed.), 809–814 (1983).

. Mehta book, page 13.

Figure 4.3

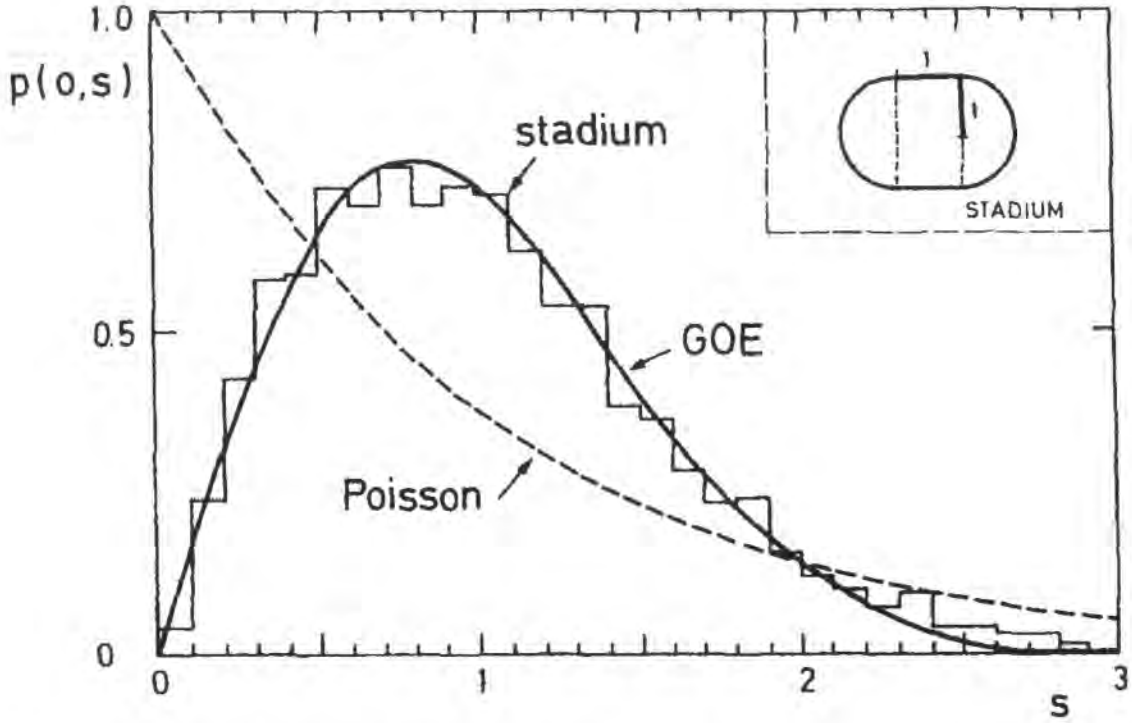


**Figure 7.7.** Empirical probability density of the nearest neighbor spacings of the possible energies of a particle free to move on the stadium consisting of a rectangle of size $1 \times 2$ with semi-circular caps of radius 1, depicted in the right upper corner. The stadium can be defined by the inequalities $|y| \leqslant 1$, and either $|x| \leqslant 1/2$ or $(x \pm 1/2)^2 + y^2 \leqslant 1$. The solid curve represents Eq. (7.3.19) corresponding to the Gaussian orthogonal ensemble (GOE), while the dashed curve is for the Poisson process corresponding to no correlations. Supplied by O. Bohigas, from Bohigas et al. (1984a).

. Mehta book, page 172.

Figure 4.4

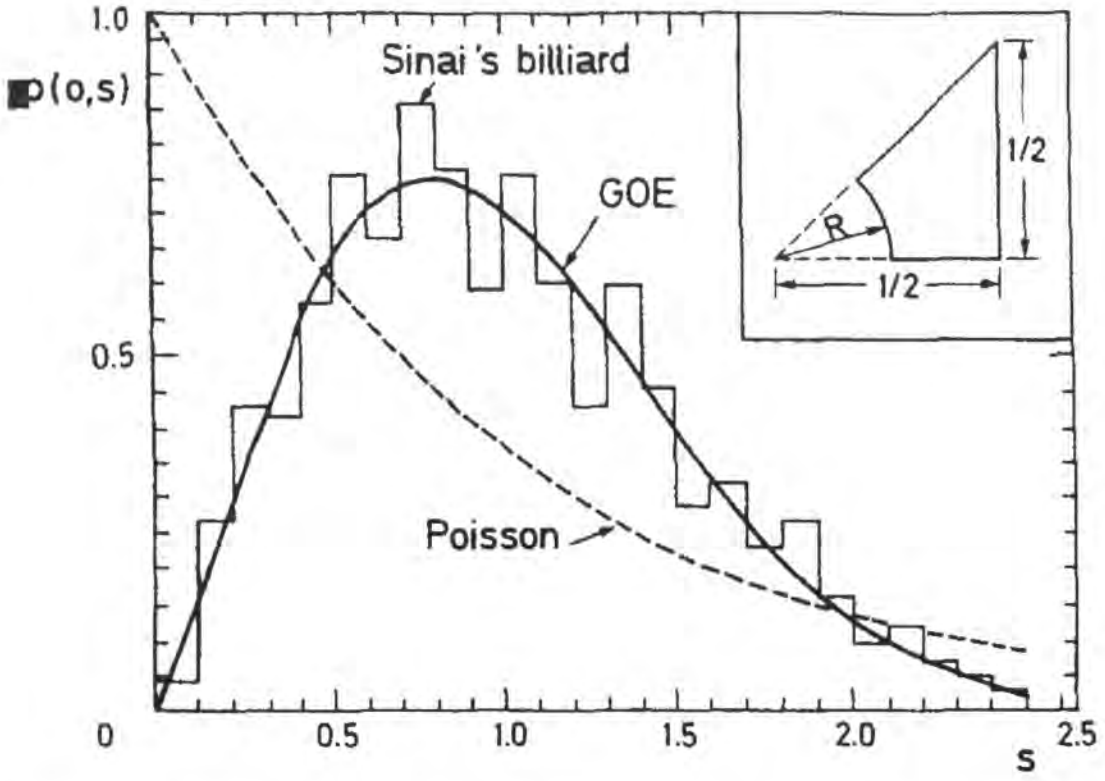


**Figure 7.8.** Same as Figure 7.7 but when the particle moves on Sinai's billiard table consisting of 1/8 of a square cut by a circular arc, depicted in the right upper corner. One may define it by the inequalities $y \geqslant 0$, $x \geqslant y$, $x \leqslant 1$ and $x^2 + y^2 \geqslant r$. Only 1/8th of the square is taken so that all obvious symmetries of the square are disposed of. Supplied by O. Bohigas, from Bohigas et al. (1984a).

. Mehta book, page 173.

Figure 4.5

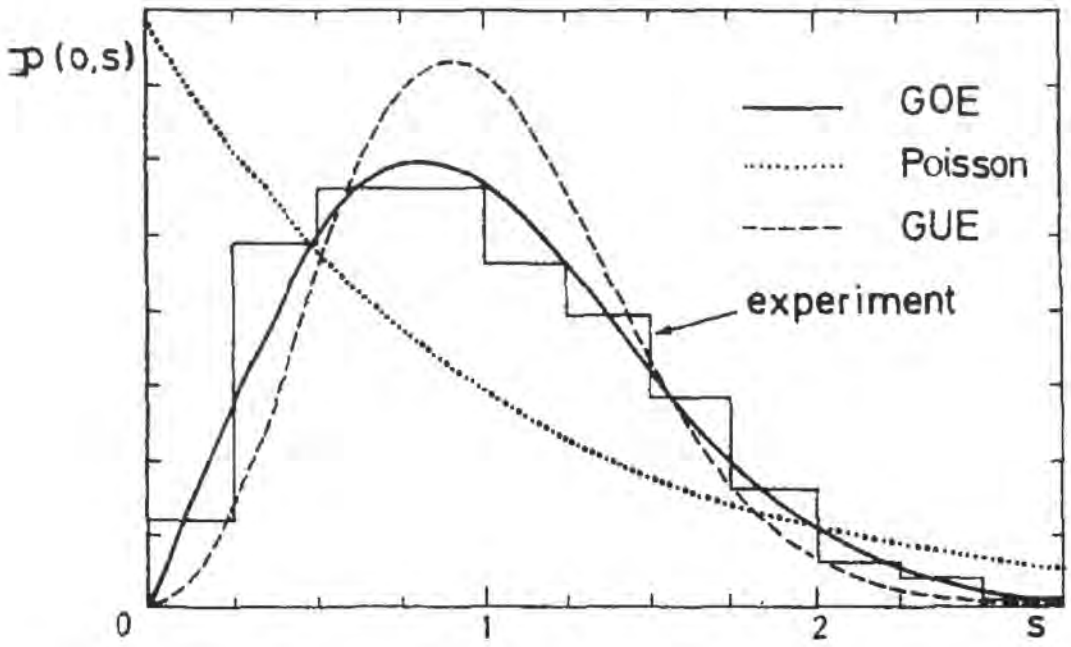


**Figure 7.9.** Empirical probability density of the nearest neighbor spacings for the ultrasonic frequencies of an aluminium block. The three curves correspond respectively to the Poisson process with no correlations, to the Gaussian orthogonal ensemble (GOE) and to the Gaussian unitary ensemble (GUE). Reprinted with permission from American Institute of Physics, Weaver R.L., Spectral statistics in elastodynamics. *J. Acoust. Soc. Amer.* 85 (1989) 1005–1013.

. Mehta book, page 173.

Figure 5.1

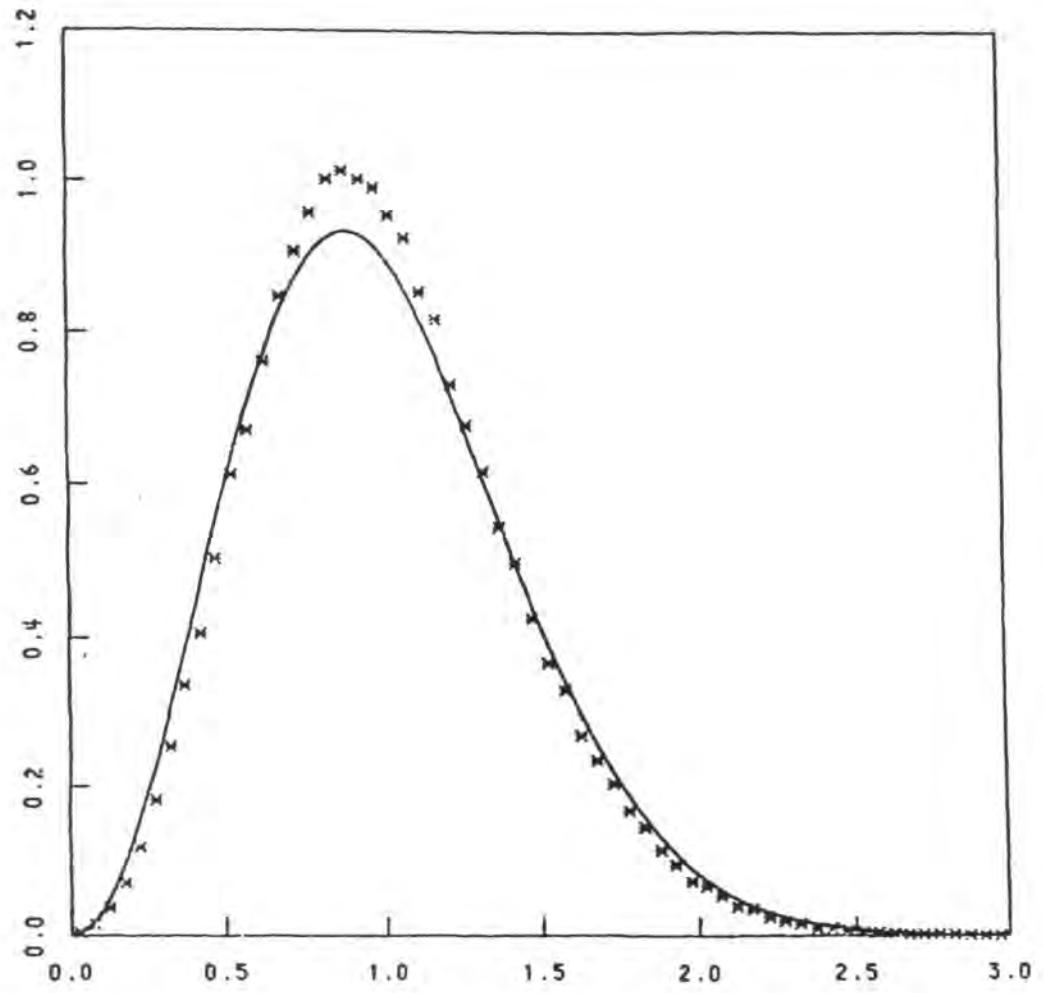


**Figure 1.12.** Plot of the density of normalized spacings for the zeros $0.5 \pm i\gamma_n$, $\gamma_n$ real, of the Riemann zeta function on the critical line. $1 < n < 10^5$. The solid curve is the spacing probability density for the Gaussian unitary ensemble, Eq. (6.4.32). From Odlyzko (1987). Reprinted from "On the distribution of spacings between zeros of the zeta function," *Mathematics of Computation* (1987), pages 273–308. by permission of The American Mathematical Society.

. Mehta book, page 24.

Figure 5.2

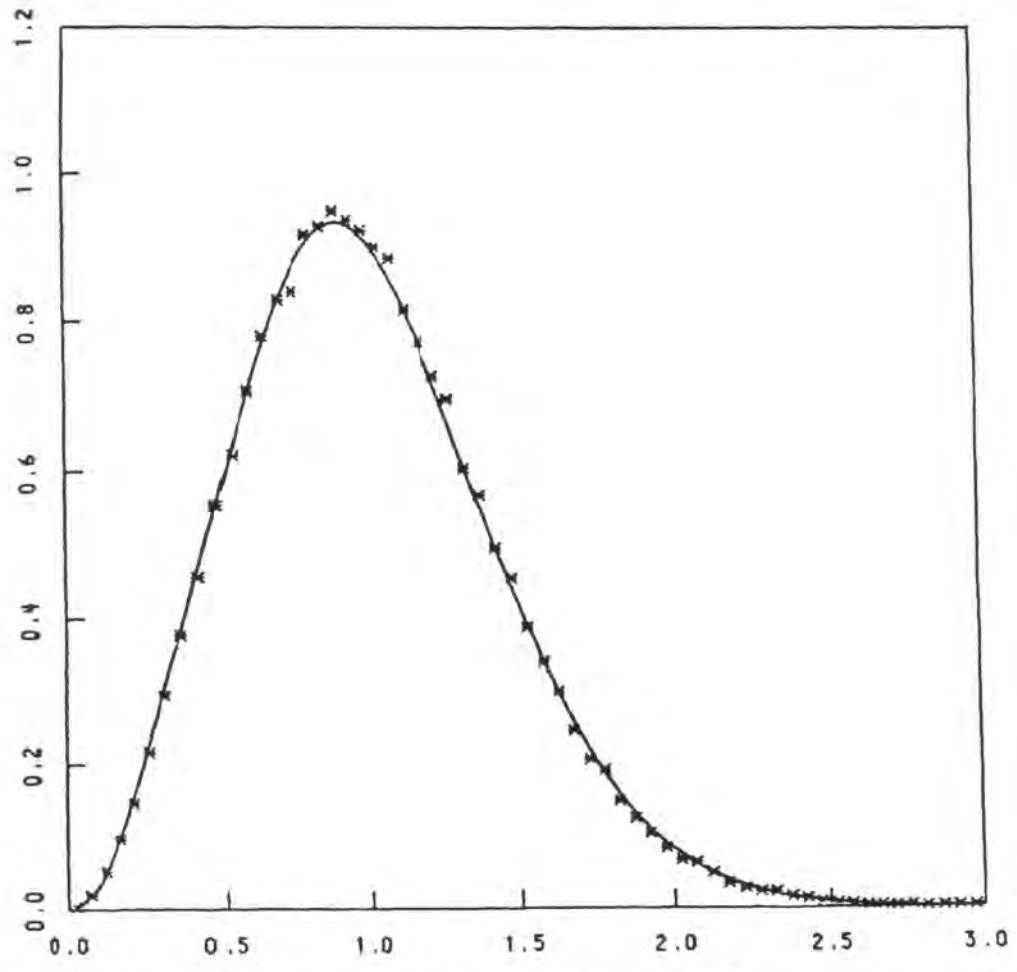


**Figure 1.13.** The same as Figure 1.12 with $10^{12} < n < 10^{12} + 10^5$. Note the improvement in the fit. From Odlyzko (1987). Reprinted from "On the distribution of spacings between zeros of the zeta function," *Mathematics of Computation* (1987), pages 273–308, by permission of The American Mathematical Society.

. Mehta book, page 25.

Figure 5.3

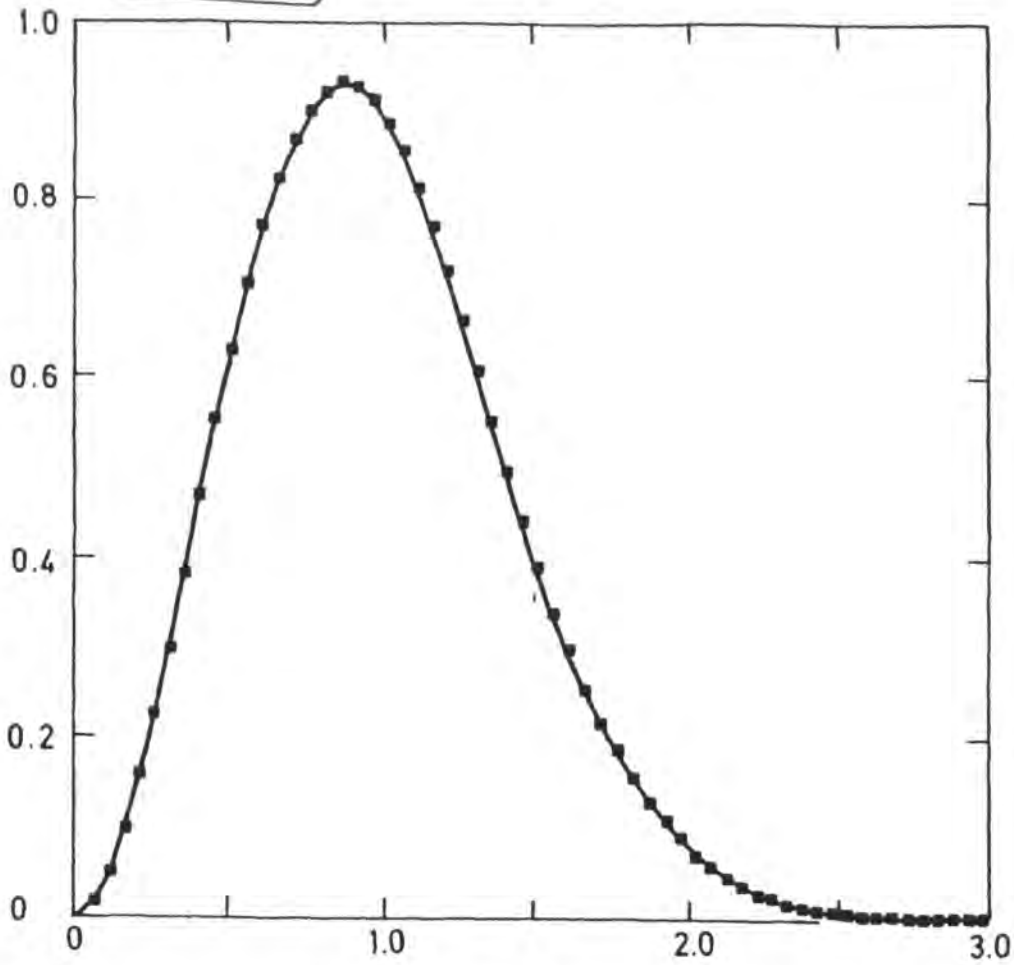


**Figure 1.14.** The same as Figure 1.12 but for the 79 million zeros around the $10^{20}$th zero. From Odlyzko (1989). Copyright © 1989, American Telephone and Telegraph Company, reprinted with permission.

. Mehta book, page 26.

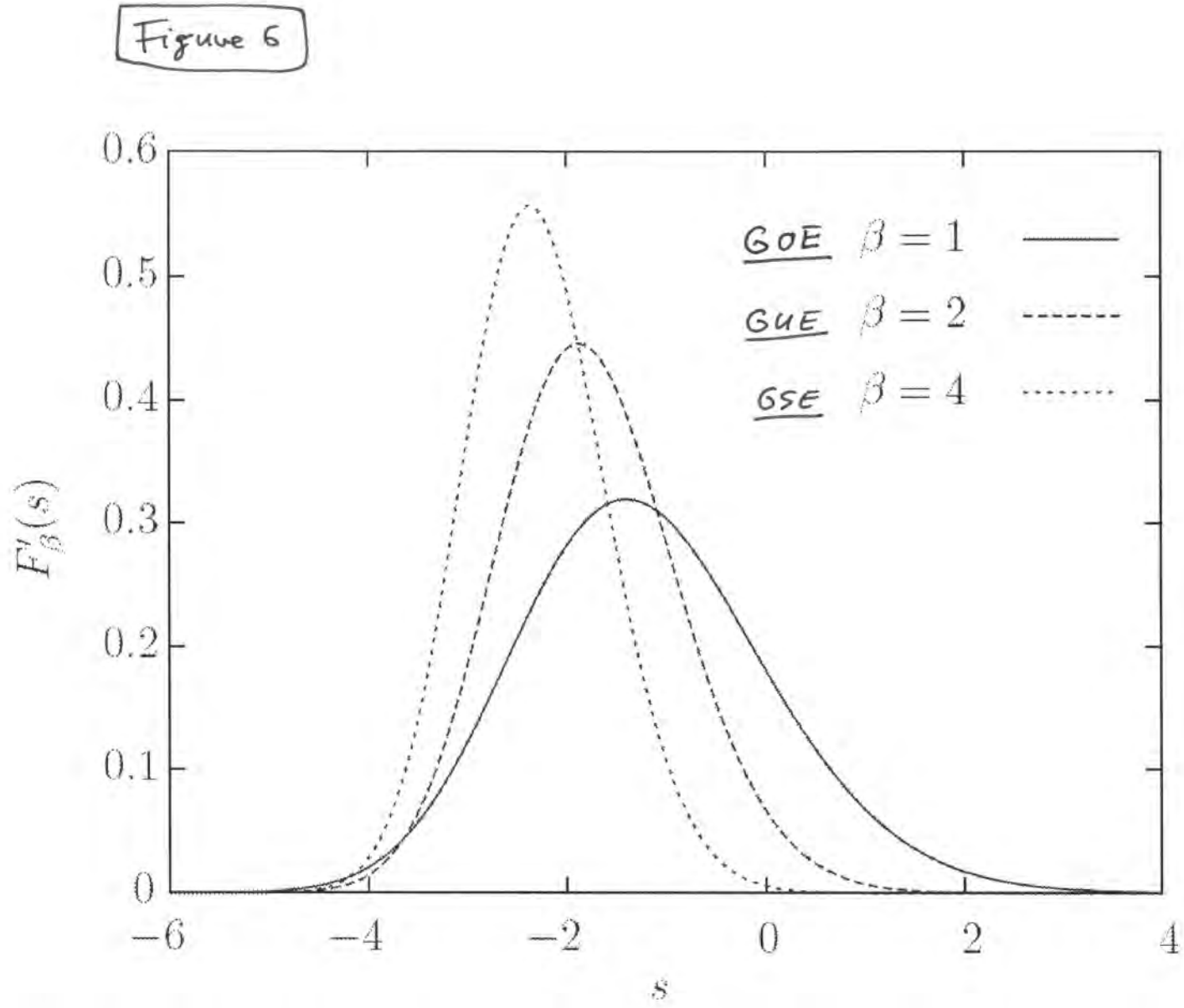


**Figure 3.1:** Probability densities of the Tracy-Widom distributions generated using [80].